ON THE UNEXPECTEDLY LARGE EFFECT OF THE RE-VAPORIZATION OF THE CONDENSATE LIQUID FILM IN TWO TESTS IN THE PANDA FACILITY REVEALED BY SIMULATIONS WITH THE GOTHIC CODE

Michele Andreani[*]
Laboratory for Thermal-Hydraulics
Paul Scherrer Institut (PSI), Switzerland

Domenico Paladino
Laboratory for Thermal-Hydraulics
Paul Scherrer Institut (PSI), Switzerland

Tom George
Numerical Applications, Inc. (NAI),
Richland, WA, USA

ABSTRACT

The recently concluded OECD SETH project included experiments on basic flows and gas transport and mixing driven by jets and plumes in the multi-compartment geometry (two large, connected vessels) of the PANDA facility, which have been simulated with the advanced containment code GOTHIC. The two experiments considered here featured injection of saturated steam in one vessel and venting from the second vessel, both being initially filled with pure air. In these two tests steam was injected at different positions. In both tests, condensation produced a liquid film on the walls in the region above the injection. For these tests the analyses with GOTHIC provided strong indications that the key phenomenon for the simulation was the re-vaporization of the condensate film, and more precisely the amount of run-down liquid which flows into the lower part of the vessel, its velocity and its re-vaporization in that region. The unexpectedly large role played by the liquid film suggested a review of the modeling issues associated with the simulation of run-down condensate. It was concluded that important gaps exist in the knowledge of several fundamental processes, which should be considered in future theoretical and experimental work related to containment thermal-hydraulics.

1 INTRODUCTION

During a postulated Loss of Coolant Accident (LOCA), a mixture of liquid and steam (later only steam) is released into the containment. The steam is typically strongly buoyant and rises to the upper part of the containment, flowing through the apertures between compartments. Due to the thermal interaction between steam and initially cold structures substantial condensation occurs, with the formation of liquid films. In a fully open geometry, films would only form in the dome and along the external walls of the containment. Depending on the break location and the geometry of the coantainment, however, films could also form along the walls of various compartments. In a dry containment, depending on the rate of downwards propagation of the steam-rich region in the steam-air ambient, the liquid film could flow into regions where local steam concentration is still low and its partial pressure is below the saturation value. Under these circumstances, the liquid would re-evaporate. If the liquid flows into a compartment where the walls are hotter that the liquid film, this would result into an enhanced evaporation rate. Due to the cooling effect of re-evaporating liquid, interest also exist for the mitigating effect of this phenomenon in the evaluation of the operability of safety-class electric equipment in a superheated ambient. In this respect, for conservative calculations the re-vaporisation rate must be limited (NUREG-0588, 1980). To simulate these effects (and also the films formed due to the injection of spray water), most containment codes include models of varying sophistication to simulate the transport of condensed water within the containment building, and the effect of its re-evaporation in regions of lower steam concentration. Some codes include models to

[*] Corresponding author

track the liquid films that form on the structures at various locations and flow to lower elevations in the containment. In general, in the evaluation of accident scenarios as well as of integral tests, which include a number of interacting processes, the specific effect on the transients of the liquid films cannot be separated from the effect of other, usually considered prevailing, phenomena. The adequate treatment of the transport of liquid films and the associated heat/mass transfer is therefore seldom in the focus of the analysis, and no specific assessment of the model used and its effect on the transient is made. However, for two tests in the OECD SETH series in the PANDA facility (Dreier et al., 1996; Auban et al., 2005) discussed here, the analyses below provided strong indications that the re-vaporization of the liquid film had an unexpectedly large effect on the transients.

The recently concluded OECD SETH project (de Cachard et al., 2007) was the framework for experiments on basic flows and gas transport and mixing driven by jets and plumes in a multi-compartment geometry (two large, connected vessels), and the test matrix included a few experiments with condensation. These experiments have been analyzed with the advanced containment code GOTHIC (2006), and the summary of the main results have been presented elsewhere (Andreani et al., 2008). In this paper, the specific role of the liquid film in two of these tests and the modeling challenges resulting from the analysis with GOTHIC are discussed in detail. The scope of the present paper is not to discuss the specific modelling features of GOTHIC, but rather to emphasize the role played by a flowing condensate liquid film on the gas distribution in a compartmented geometry and the modeling challenges that follow from this observation.

1.1 The OECD SETH Project

The SETH project (Yadigaroglu et al., 2003; de Cachard et al., 2007) was performed under the auspices of the OECD with the participation of 15 countries. The component of the project related to safety issues in the containment of a nuclear reactor consisted of twenty-four tests performed in the large-scale facility PANDA. In these tests basic flows and gas transport and mixing driven by jets and plumes in a multi-compartment geometry have been investigated. The tests have been designed to provide an adequate database for basic assessment of CFD and advanced LP codes. Most of the tests do not include condensation to allow investigation of transport processes without the complication of phase change. However, four tests (identified in the SETH project as Tests 4bis[1], 9bis, 21bis and 25), were performed with initial and boundary conditions that resulted in substantial condensation rates. The tests where the influential role of the liquid film was recognized were Tests 9bis and 21bis.

1.2 The PANDA Facility and Configurations for the Two Tests

PANDA is a large-scale thermal-hydraulics test facility designed and used for investigating containment system behaviour and related phenomena for different ALWR designs and for large-scale separate effect tests. The containment compartments and the Reactor Pressure Vessel (RPV) are simulated in PANDA by six cylindrical pressure vessels (Fig. 1). The height of the facility is 25 m, the total volume of the vessels is about 460 m^3 and the maximum operating conditions are 10 bar and 200 ^oC. The RPV is electrically heated with a maximum power of 1.5 MW. For the SETH tests, only parts of the facility were used. The experiments considered in this work were carried out in a large (about 180 m^3 total volume) multi-compartment volume consisting of the two identical vessels (referred to as Vessel 1 and Vessel 2 in the SETH project), 8 m in height and 4 m in diameter, connected by a large Interconnecting Pipe (IP), 1 m in diameter. Fluid was injected in Vessel 1, and the gas distribution and the propagation of the stratification in both vessels were measured. The PANDA instrumentation includes more than 1000 sensors allowing measurements of fluid and wall temperatures, absolute and differential pressures, flow rates, heater power, gas concentrations and flow velocities. The measurement sensors are implemented in all the facility compartments, in the system lines and in the auxiliary systems. The number of sampling lines used for gas concentration measurements in each test was 38. A thermocouple is placed close (within a few millimeters) to each gas sampling port so that gas concentration and temperature measurements are available at the same spatial location. The geometrical configurations for the two tests discussed here are also shown in Figure 1. In Test 9bis,

[1] The three tests for which similar tests without condensation (starting from different thermodynamic conditions) have also been executed are identified with the "bis" suffix.

saturated steam was injected at low velocity from a nozzle penetrating the vessel wall at about 1.8 m above the bottom of the vessel (Fig. 3). The low-momentum injection resulted in a plume confined on one side by the wall ("near-wall" plume). Due to the large dilution of the steam before approaching the wall, condensation started late in the transient. More information on the experimental results can be found in Paladino et al. (2006). In Test 21bis, saturated steam was injected from a vertical pipe aligned with the axis of the vessel, with the exit section at 6 m above the bottom of the vessel (Fig. 4). The low-momentum injection resulted in a vertical plume nearly unconfined in the transverse direction ("free" plume).

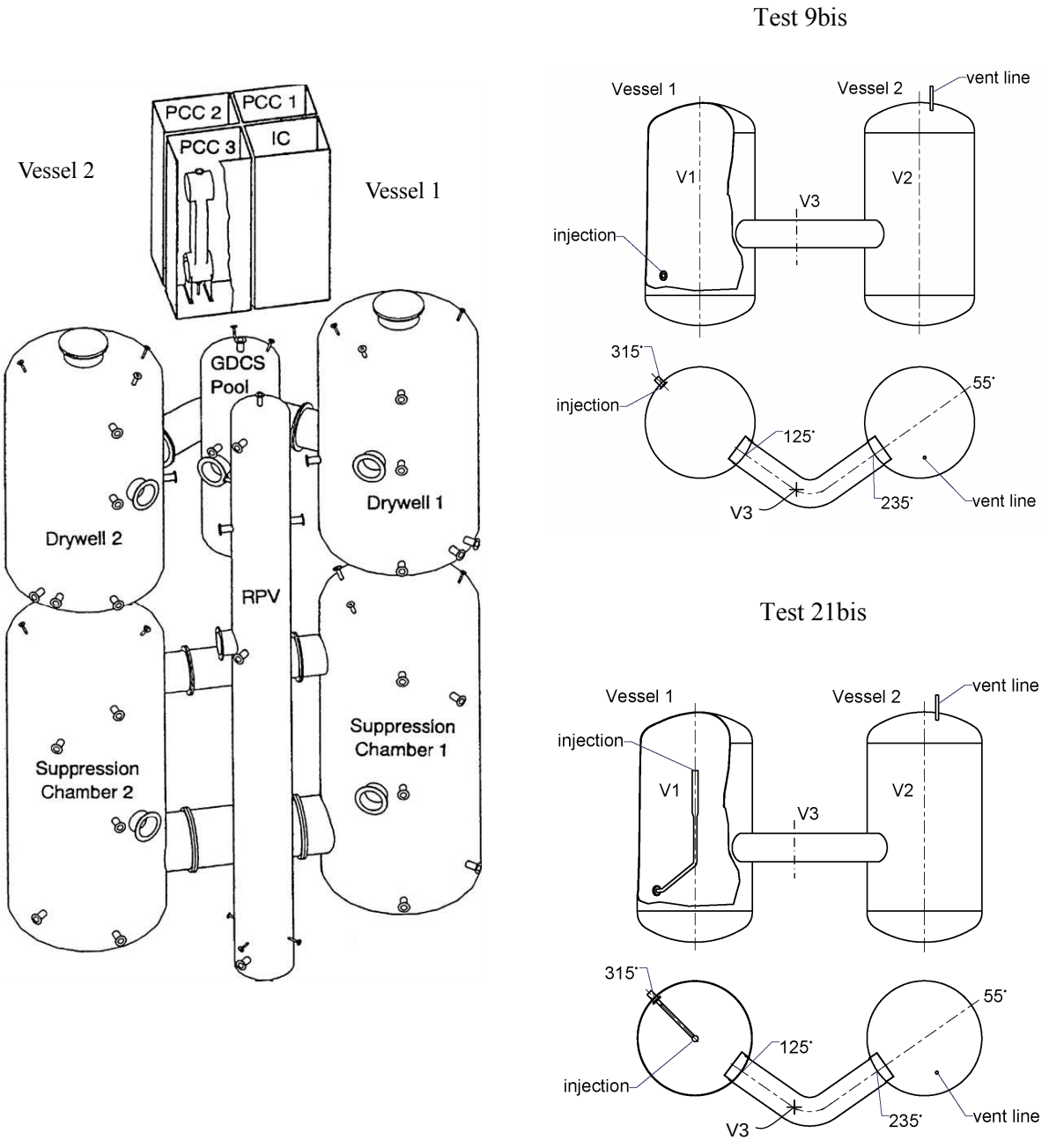

Figure 1. The PANDA facility (left) and the configurations of the upper vessels (Vessel 1 and Vessel 2) for Tests 9bis and 21bis (right).

Due to the short distance between injection and the vessel dome, condensation started early in the transient. More information on the experimental results can be found in Zboray et al. (2006). The pressure was maintained constant during the tests, pressure control being obtained by venting to the atmosphere from a nozzle in the dome of Vessel 2. The fluid and walls were in thermal equilibrium at the beginning of the tests, at a few tens degrees below saturation temperature. The duration of both tests was 2 hours, and the injection flow rate (practically constant) was the same in the two tests.

In these two tests, the effect of re-vaporisation resulted to be especially strong due to both initial conditions (wall temperature) and geometry (interconnected vessels). In fact, due to the large temperature differences between the injected saturated steam and the walls, large condensation rates occurred in the upper part of the fluid-receiving vessel. This produced a liquid film which moved downwards faster than the expansion rate of the steam-rich region, as most steam was consumed by condensation. The liquid thus reached the lower region when undersaturated conditions still prevailed, and re-evaporated. An additional contribution to the delay in the propagation of the steam in the fluid-receiving vessel was the transfer of gas (but not of liquid) into the second vessel. Finally, the high initial temperature of the wall (nearly the same over the entire height of the vessels) initially increased the evaporation rate of the condensate film as this was at rather low-temperature when first descended in the lower region, because it had been formed in the upper region when the steam content was still small and consequently the saturation temperature was still low.

The conditions that were realized in these two experiments, although they tend to overemphasize the role played by the condensate film, are representative of the complex physics that can occur in a compartmented containment and are therefore relevant for safety issues related to the distribution of steam and its effect on the transport of other gases and aerosol components produced during various accident scenarios.

2 THE GOTHIC CODE

GOTHIC is a general-purpose, thermal-hydraulics computer program for design, licensing, safety and operating analysis of Nuclear Power Plant (NPP) containments and other confinement buildings. The thermal-hydraulics module is based on a two-phase, multi-fluid formulation, and solves separate conservation equations for mass, momentum and energy for three fields: a multi-component gas mixture (including steam), a continuous liquid, and droplets. In addition, mass balances are solved for each component of the gas mixture.

The phase balance equations are coupled by mechanistic models for interfacial mass, energy and momentum transfer. GOTHIC includes a full treatment of the momentum transport terms in multi-dimensional models, with optional models for turbulent shear, and for turbulent mass and energy diffusion. The options for turbulence are the mixing-length model and several variants of the k-ε model. The hydraulic model of GOTHIC is based on a network of computational volumes (one, two or three-dimensional) connected by flow paths.[2] In contrast to standard CFD packages, GOTHIC does not have a body-fitted coordinates capability, and the code uses boundary-layer correlations for heat, mass and momentum exchanges between the fluid and the structures, rather than attempting to model the boundary layers specifically. The subdivision of a volume into a multi-dimensional grid is based on orthogonal co-ordinates with cell and flow area porosities: the actual geometry of volumes with curved surfaces (e.g., a cylindrical vessel) can be represented, however, by full or partial blocking of cells to define the porosity factors. Energy exchange between fluid and solid structures (referred to as thermal conductors) is accomplished using a general model for heat transfer between structures and steam/gas mixtures, or between structures and liquid. Several heat transfer modes are represented, including forced and free convection, boiling and condensation, and radiation. The numerical solution of the transport equations is based on a semi-implicit method. The method is first-order in time. For

[2] For connecting subdivided volumes the pre-processor permits the grouping of multiple flow paths in '3-D connectors'. This feature has been used only for the latest modifications of the original PANDA model.

the space-discretisation of the advection term both a first-order upwind and a bounded second-order method are available. The 3-D capabilities of GOTHIC, to simulate basic flows of interest for containment analysis, have been extensively investigated (e.g. Andreani et al., 2003), and many of the applications to containment analysis include 3-D models. The version of the code used in the present analysis is GOTHIC 7.2a(QA).

3 NODALISATIONS AND MODELS USED FOR THE SIMULATIONS

Figure 2 shows the GOTHIC model used for Test 21bis, the model for Test 9bis being practically the same, with the only difference that the injection line (flow path 5) is horizontal and ends at short distance form the vessel wall. The RPV (steam source) is represented by a boundary condition (1F) with prescribed flow rate and temperature for the injected steam. The vent is represented by a flow connection (flow path 56) to a prescribed pressure boundary condition. The model includes a 3-D representation for Vessels 1 and 2 (5s and 7s, respectively) and the IP (6s). The two vessels are connected to the IP by multiple flow paths. The small volume (8s) on the top of the Vessel 1 represents the large man-hole and is connected to the vessel by a 3-D connector. This was included for the simulation of Test 21bis only, as in this test the jet was directed towards the dome of the vessel. The mesh that has been used for the reference calculations, referred to as "standard mesh", is shown in the left part of Fig. 3 (where the IP is somewhat enlarged for readability), and some details of the subdivision are presented in Table 1. In this model the actual geometry of the vessel (a cylinder, with lower and upper header having ellipsoidal shape) has been replaced by parallelepiped boxes. It can be observed that the subdivision of Vessel 1 is somewhat finer than that for Vessel 2 as it was expected that the most important phenomena would be driven by the injected flow in Vessel 1 and an adequate resolution would be required for capturing some details of flow and heat transfer close to the injection. Details such as the flow obstruction caused by the injection pipe (different for the various tests) and the protrusion of the IP into the Vessels 1 and 2 have been represented. The nodalization used for both Vessels is still rather coarse (using about 23'700 cells) and not representative of the detail that would be required for a full CFD analysis. The most obvious consequence of the simplification to represent the vessels as boxes (implying an alteration of the volume distribution with elevation) is that the filling time of the upper dome in Test 21bis could not be represented accurately. The simulations for this test were therefore run also with a different geometrical representation, closer to the actual one, which is shown in Fig. 8. It can be observed that the vessels consist of a cylindrical section, and two hemispherical (lower and upper) headers. The man-hole is represented for both vessels. The IP is also

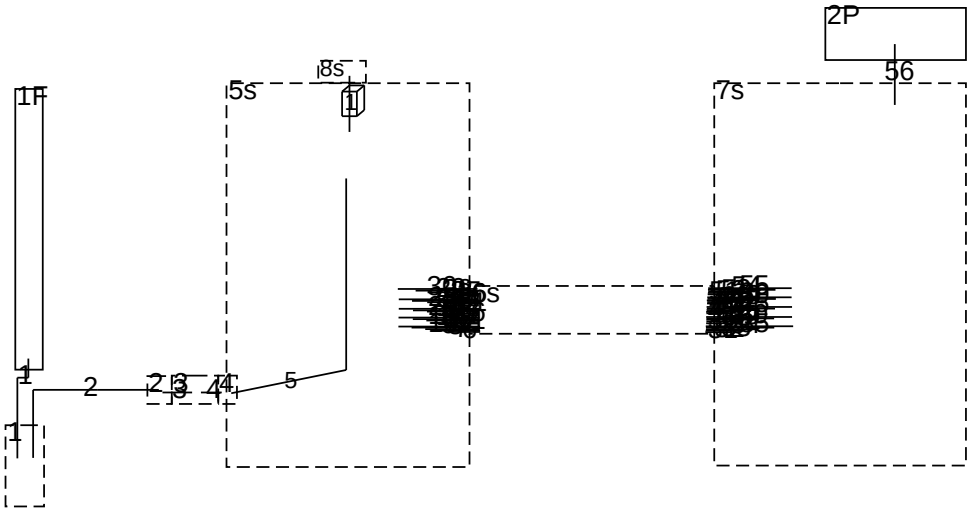

Figure 2. General model used for the simulations.

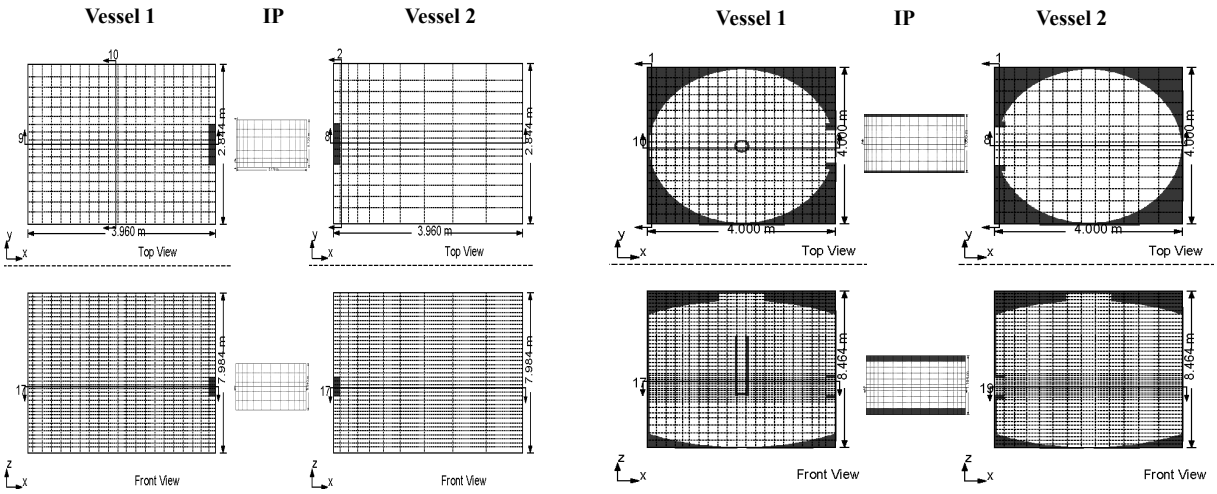

Figure 3. Nodalisation of upper vessels and IP used for the simulations of both tests (left) and refined nodalisation for Test 21bis (right).

represented more faithfully with a straight pipe, of cylindrical section (not shown). A more complete discussion of the features of this improved mesh is given in Andreani et al. (2008).

The metal walls of the PANDA vessels have been fully represented, to take into account the heat capacity of the structures. The insulation of the vessels has not been included in the model because of the small heat capacity, and the small heat losses to the environment have been implemented in the model by prescribing the average heat flux as a function of the wall inside temperature. The standard (high-Reynolds) k-ε turbulence model was used for Vessels 1 and 2 and the IP. Previous simulation for large-scale vessels (Andreani, 2003) showed that this model provides more accurate results in relation to mixing processes than other variants (e.g. RNG). Also calculations of earlier PANDA tests were successful using this model and a coarse mesh.

An important aspect of the coarse mesh used for the analyses is that it cannot resolve the condensate liquid film flowing down the walls. Under these conditions, the liquid would migrate towards the interior cells far from the structures. To prevent unphysical diffusion of liquid, GOTHIC includes in the transverse momentum equation an "adhesion force", which keeps the liquid on the walls. The wall shear is calculated using a correlation for wall friction, rather than the more typical CFD approach of integration of the momentum equations to the wall and the use of a wall function. How well this approach can represent the flow of a thin liquid film on a vertical wall is discussed in Section 5. For heat transfer between fluid and structures, there are basically two main options in GOTHIC for simulating condensation processes: the DIRECT option and the FILM option.[3] Therefore, sensitivity studies have been performed using these two options, which are briefly illustrated below.

Table 1. Meshes used for the simulations in the X;Y;Z directions.

Mesh	Geometry	Vessel 1	IP	Vessel 2	Tests
"Standard"	boxes	25;17;41	12;5;5	10;15;40	9, 21
"RG" (Real Geometry)	Cylinders +hemispherical domes	21;19;43	15;5;10	13;15;48	21

[3] The Tagami model can also be selected, but this model, fully empirical, is based on a blowdown to a single lumped parameter volume, and is thus of no use for 3-D analysis.

DIRECT option: condensation occurs at the wall (dry-wall model), and is calculated by a correlation (Uchida or Gido-Koestel) or by an advanced diffusion layer model (**DLM-FM**), which was developed for GOTHIC. The diffusion layer model (which is the recommended choice as a result of the extensive validation of the model) calculates the condensation rate and sensible heat transfer rate using heat/mass transfer analogies. It includes options for the formation of mist in the boundary layer and heat and mass transfer enhancement due to roughness of the condensate film. The model is applicable to the full range of steam gas mixtures in forced and free convection. An important limitation of this model is that it considers heat transfer between wall and liquid only if thermodynamic conditions permit condensation. If the wall is hotter than the liquid, no heat transfer between wall and condensate occurs. The direct option was used for all the basic calculations in this work.

FILM option: this option attempts a more mechanistic treatment of heat/mass transfers, considering the film of liquid (wet-wall model). The wall is split into wet and dry portions based on the available water for film coverage. Convection to the vapor is calculated to the vapor phase for the dry portion and to the liquid for the wet portion. Also, if the wall is cold enough, condensation on the dry portion is calculated using Uchida or Gido-Koestel or if it is hot enough boiling is calculated for the liquid portion. Otherwise all phase change occurs at the liquid/vapor interface using the convective heat transfer coefficients on either side of the interface and the analogous mass transfer coefficient on the vapor side.

It will be seen that the most obvious result of the differences between the two models is the amount of re-vaporisation of a liquid film draining along hot structures.

4 RESULTS

In this work, only the results related to the role of the re-evaporating condensate film will be presented, since the discussion of the general results have already given by Andreani et al. (2008). For the sake of clarity of presentation, the overall results for the two tests are also briefly summarized.

4.1 Test 9bis

The steam injected accumulated first in the upper part of the vessel and then propagated downwards, producing a slowly moving stratification front. When the front reached the level of the IP, part of the steam was transported into Vessel2, with the remaining steam flowing into the lower part of Vessel 1. At about 2’900 s the steam concentration in the upper part of Vessel 1 reached saturation conditions and condensation started. In Vessel 2 this happened somewhat later (around 3’800 s). The gas distribution in Vessel 1 resulting from these flow and condensation processes was generally well predicted by the code. The vertical steam distributions in the IP and Vessel 2 are also in reasonably good agreement with data. The predicted results in both vessels are in very good agreement with data at all elevations before condensation occurs, whereas the stratification front below the injection is too sharp after condensation starts. It is believed that the smaller concentration gradient across the downward propagating stratification front observed in the test is due to the redistribution effect caused by the re-evaporation of the liquid flowing below the front from the upper part of the vessel, which cannot be predicted accurately by the code, as discussed below.

The experimental evidence that liquid condensed in the upper part of the vessel re-evaporated in the lower part is provided by the fluid temperature time histories at the various elevations. Fig. 4 shows the measured gas temperatures at three elevations along the axis of Vessel 1. It can be observed that above the injection the gas remained at nearly the same temperature for a long time, and increased after 2’900 s, starting from the higher elevations. Around this time, the steam partial pressure close to the structures exceeds the saturation pressure at wall temperature, and condensation occurs, starting from the higher elevations. The wall condensation rate is less than the steam injection rate and the steam concentration in the bulk fluid continues to increase. The local steam partial pressure in the centre of the vessel reaches the saturation value (Paladino et al., 2006) at the local temperature, and the gas temperature increases along the saturation line from then on due to condensation (fog or mist

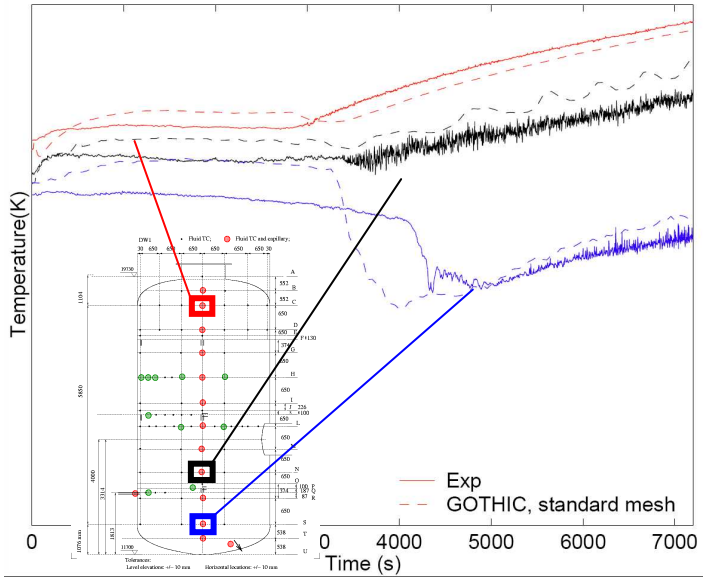

Figure 4. Measured and calculated gas temperatures at three elevations along axis of Vessel 1.

formation) in the bulk fluid. Below the injection, however, the accumulation of steam transported from above is much slower, and the steam partial pressure remains below saturation much longer. Under these conditions, liquid falling from above re-evaporates and the saturated steam produced, which is colder than the ambient fluid (because the partial pressure is still low), causes the fast temperature drop in the lower header observed in Fig. 4. Eventually, saturated conditions are reached also in the lower header and the fluid temperature increases also there. Figure 4 shows that the simulation with GOTHIC captures very well the temperature trend above the injection, but grossly underpredicts the time of the temperature drop in the lower header. This disagreement can be explained by considering the calculated liquid distribution and the interfacial mass transfer rate in the node closest to the wall at different elevations. Figure 5 shows the liquid volume fraction contours at two different times shortly after the onset of condensation in Vessel 1. It can be observed that the wall liquid film has propagated to the elevation of the lower header within less than 200 s. At this time the interfacial mass transfer (plot in the centre of the figure) in the lower header is positive, indicating evaporation, while is condensation above there injection. This combined information suggests that the measured gas temperature drop is indeed caused by the re-evaporation of the condensate liquid film and that the inability of the code to predict the temperature trend below the injection is due to the overprediction of the run-down velocity of the liquid film. Attempts to improve predictions by refining the mesh did not produce any significant improvement. On the other hand, the use of the FILM heat

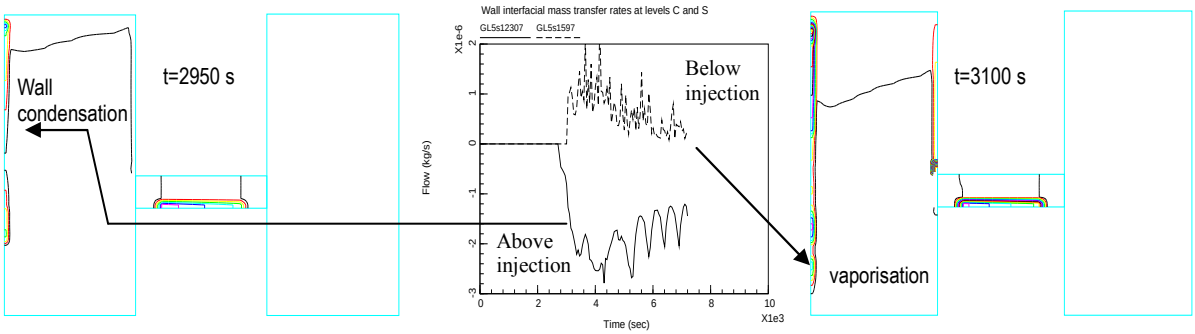

Figure 5. Calculated liquid volume fraction distribution at two different times (left and right), and interfacial mass transfer rate in the node closest to the wall (centre).

transfer model option produced a smaller temperature decrease without, however, any change in the timing of this drop. In principle, the sudden gas cooling at low elevations might have been caused by evaporation of droplets formed from the fog in the upper part of the vessel. However, the amount of the droplet phase created in the simulation was very small and parametric studies on the input parameters that control the drop formation from fog showed no effect. It was therefore attempted to artificially delay the downward motion of the liquid film, just to obtain confirmation that the excessive liquid film falling speed could be the reason for the poor temperature predictions below the injection. Figure 6 shows the results of various calculations, including the effect of a vertical blockage along the wall, simulating a tray (curb) that collects all the descending liquid, and of increased wall friction. It is observed that either collecting the liquid or imposing very high wall friction results in improved agreement with the measured temperature, giving evidence that the re-evaporation of the liquid film is the probable physical mechanism controlling the gas temperature drop below the injection.

4.2 Test 21bis

The main phenomena in Test 21bis are basically the same as in Test 9bis, with the only notable exception that the largest condensation rates are in the dome of Vessel 1 and the steam concentration in Vessel 2 remained below levels that would permit condensation. Details of the experiment can be found in Zboray et al. (2007). The test was simulated using both geometrical representations presented in Section 3. Since the results of the simulations were quite close to each other in relation to the main aspects of the transient, only the results with the realistic model ("RG mesh") will be discussed here. As discussed in the companion paper (Andreani et al., 2008), simulations using the DIRECT heat transfer mode showed major discrepancies with the measurements, while the FILM option resulted in better predictions of the steam distribution. In particular, the stratification in Vessel 2 is completely different for the two heat transfer options, with the DIRECT option resulting in an axial profile reverted with respect to the measured one. Figure 7a shows the steam fraction distribution and the the velocity vectors at 2'000 s in the (folded) vertical plane containing the axes of the vessels and of the IP for the case with DIRECT heat transfer. Figure 7b shows the corresponding results obtained using the FILM option. In the former case steam is flowing from Vessel 1 into the lower part of the IP, creating a cascade of a gas mixture containing some steam into the lower part of Vessel 2. When the FILM

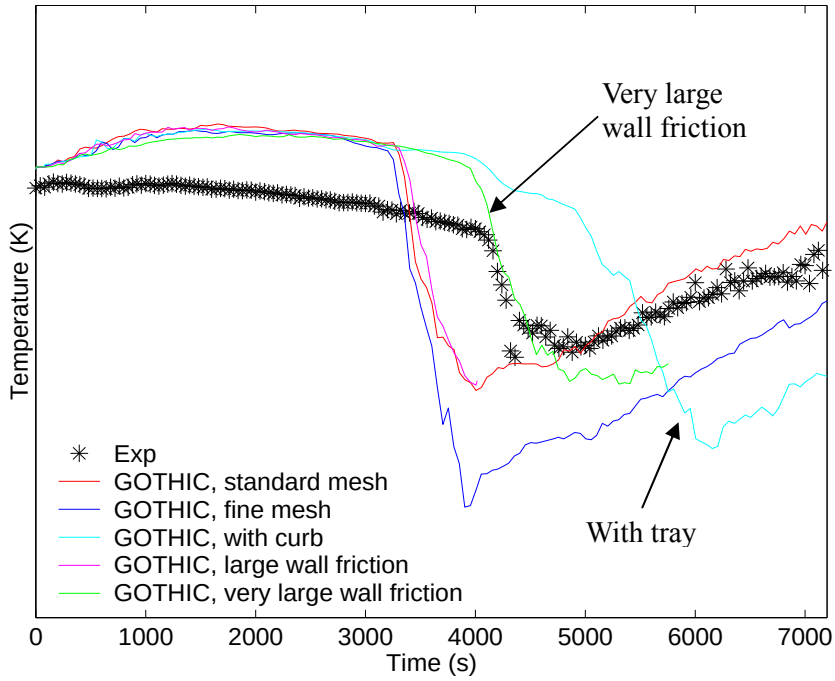

Figure 6. Parametric studies showing the effect of artificially delaying the downwards motion of the liquid film.

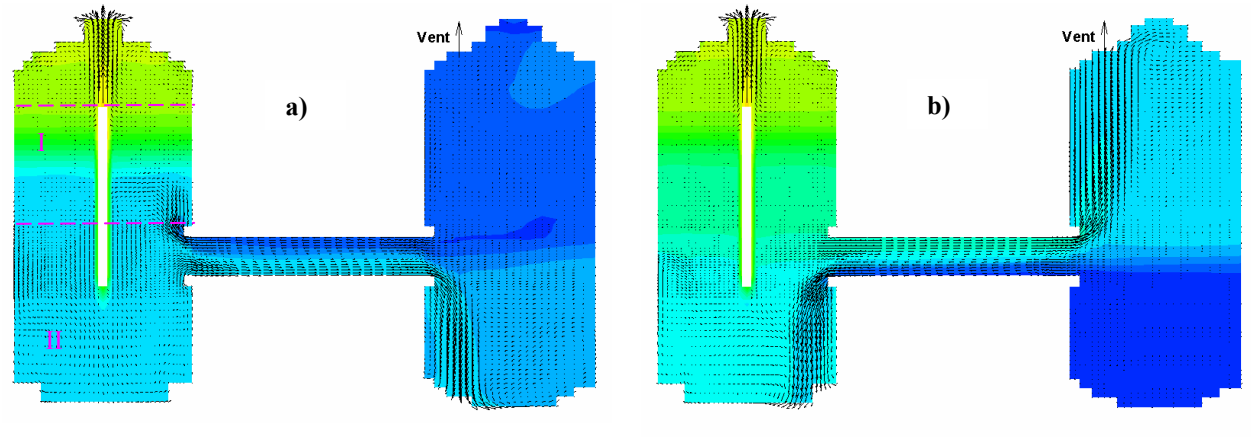

Figure 7. Steam molar fraction and velocity fields at 2'000 s calculated by GOTHIC using: a) DIRECT wall heat transfer option; b) FILM heat transfer option.

option is used, a mixture containing steam flows into the IP from the upper part of Vessel 1, and from there rises in the upper part of Vessel 2. In general, the difference in the results is considerable and to a certain extent unexpected. In this work, only these differences will be highlighted and modeling difficulties will be discussed, as the comparison with the main experimental results was already reported. In the companion paper (Andreani et al., 2008) it was argued that the reason for this large differences was the different re-vaporisation rate of the condensate liquid film using the two options. Figures 8a . 8b show the rates of vaporization and condensation (as well as the net mass transfer rate) in the region between the top of the IP and the elevation of the injection (Region I in Fig. 7), and in the region below the top of the IP (Region II in Fig.7), respectively. It can be observed that the vaporization rates calculated with the FILM model are much higher that those computed using the DIRECT option. Therefore, when the DIRECT heat transfer option is used, the liquid condensate flows downwards with little re-evaporation in the upper part of the vessel. When this liquid reaches the lower part of Vessel 1 where the steam concentraton is low due to stratification, it re-evaporates. The re-vaporisation results in the growth of a zone of colder air/steam mixture at the bottom of Vessel 1 that eventually spills over into the lower part of Vessel 2. The use of the FILM option, instead, results in substantial re-vaporisation in the upper part of Vessel 1, and a faster downwards propagation of the steam-rich region. When the bottom of this expanding zone reaches the top of the IP, warmer fluid of high steam content flows into the upper part of the IP, and creates a plume in Vessel 2.

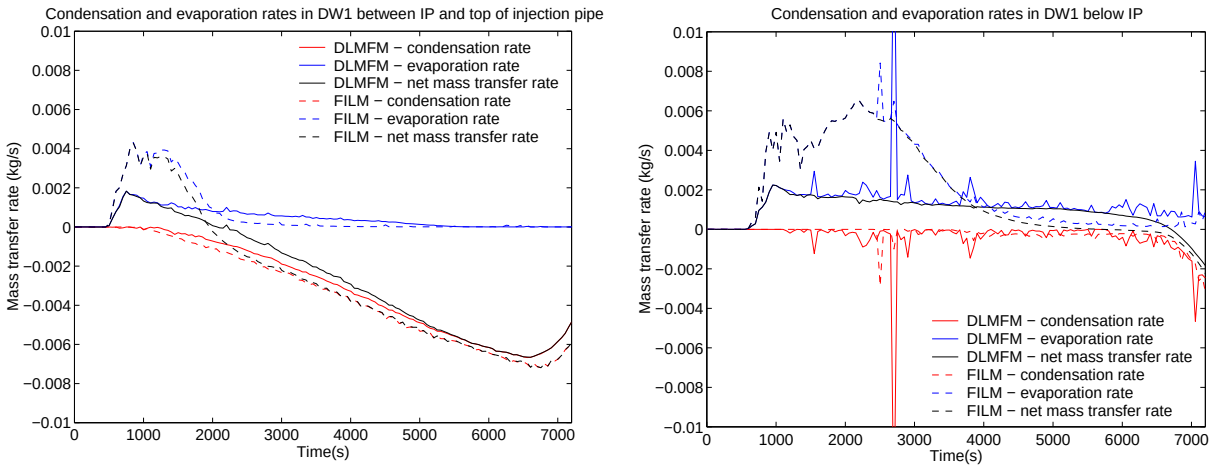

Figure 8. Total interfacial mass transfer rates in region I (left) and region II (right) in Vessel 1 (see Fig. 7) calculated using the DIRECT and FILM heat transfer options.

From the observation of the interfacial heat/mass transfer and steam concentration field, however, it is not obvious why the larger steam production in the lower part of the vessel did not lead to the same flow pattern that was realized using the DIRECT option. To understand the difference between the two simulations it is helpful to consider that the flow between the two vessels is controlled by (small) density differences, and the density depends on both steam concentration and temperature. The difference in the flow pattern in the two simulations is therefore better understood if one considers the fluid density. Figure 9 shows a sequence of four snapshots of the density distribution for the two simulations.

The calculation using the DIRECT option (left in the figure) shows that denser fluid mostly originated from the walls (although a part of it falls from the region above where re-evaporation of the liquid film starts) starts filling the lower part of Vessel 1 at around 700 s. The steam generated at the bottom of the vessel is at low temperature due to the low steam concentration and corresponding low saturation temperature. At 800 s the lower part of the vessel is completely filled with a gas/steam mixture that is denser than the fluid in Vessel 2, and the mixture flows from Vessel 1 into the lower part of Vessel 2. This pattern (which is also shown at 1'000 and 2'000 s) persists until late in the transient, when the expanding hotter fluid zone in the upper part propagates below the top of the IP.

The simulation using the FILM option shows initially the same behaviour (snapshots at 700 and 800 s), but soon (1'000 s) the expanding hotter fluid zone in the upper part of the vessel, due to the steam injection and the revaporization of the falling film, extends down below the top of the IP and buoyancy induced migration to Vessel 2. The steam generation from the revaporization of the falling film in the upper part of the vessel is at a high temperature due to the high steam concentration in this region and the corresponding high saturation temperature. Eventually (see snapshot at 2'000 s) the zone of low density (red coloured, where density is lower than in Vessel 2) disappears, and the hot, steam-rich mixture flows into the upper part of Vessels 2

From these results, it can be concluded that system behavior depends not only on the amount of re-evaporation but also where it occurs as well as on the temperature of the generated steam.

As the phenomena are quite complex and the interaction between the three fields (drops, gas, liquid) and of the fluid with the structures is the result of a number of models and empirical correlations, various parametric studies using the DIRECT option have been performed to confirm that the liquid film actually played an important role in the test. First, the bulk condensation (mist) model was deactivated; second, the drop field was removed entirely from the simulation. Both changes resulted in practically no difference. Also, a prescribed liquid re-evaporation fraction for the film did not lead to any improvement of the results. The attempt to delay the propagation of the film by imposing higher friction with the wall (as in Test 9bis) did not produce reasonable result, as also the expansion of the upper steam-rich mixture was strongly hindered. Finally, it was imposed that all the liquid present in the upper dome was converted to droplets to check if the evaporation from droplets could result in a different density distribution between the upper and lower part of Vessel 1. Different sizes of droplets were tested (1mm, 0.1 mm and 0.01 mm). Results similar to those obtained using the FILM option, and most probably realized in the experiment, could only be obtained when the prescribed size for the droplets was of 0.01 mm, and nearly complete vaporization occurred in the upper part of the vessel. On the one hand, this confirmed that the correct density distribution and flow pattern between the two vessels could only be obtained if sufficient re-vaporisation of the condensed water occurred in the upper part of the vessel. On the other hand, this parametric study suggests that the liquid flowing downwards in Vessel 1 must have been in the form of continuous liquid film, because an entrainment mechanism that produces so small droplets (10 μ) is rather unlikely to occur under the conditions of the test, where the pressure and velocities are low. Although some uncertainty remains on the role played by other liquid transport mechanisms (entrainment/de-entrainment), the parametric studies above confirmed that the run-down condensate liquid is most likely to have played a key role in Test 21bis.

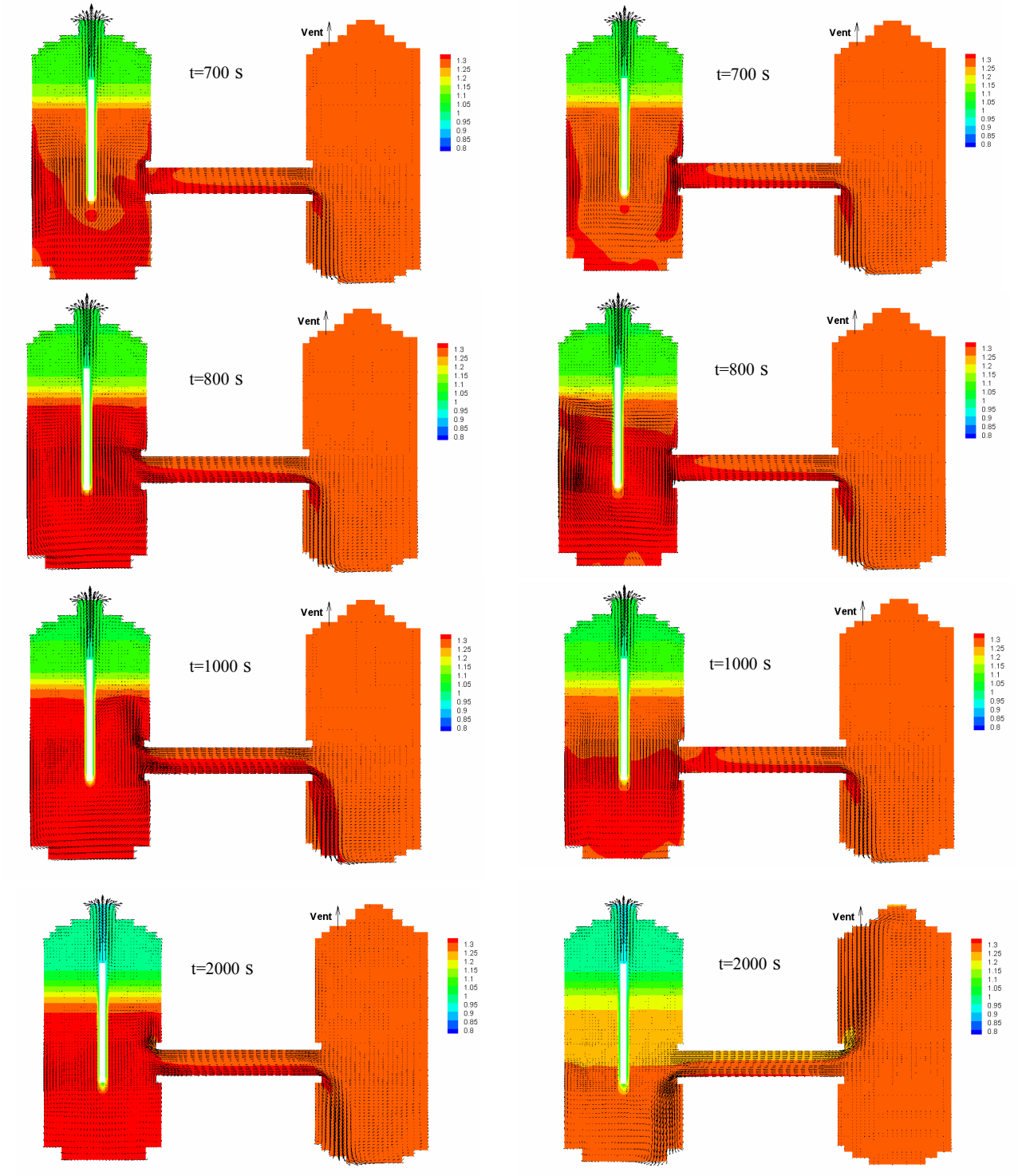

Figure 9. Snapshots of the density distribution at four different times; left: results obtained with the DIRECT option; right: results obtained with the FILM option.

5 DISCUSSION

The problems identified in the analysis of the two tests discussed above are related to two (connected) modelling issues, namely the hydraulics of a thin film and its heat transfer with the wall. These effects

had different relative importance in the two tests. In Test 9bis, the speed of the falling liquid film controlled the gas temperature drop, whereas the heat transfer controlled the steam distribution and the density driven flows between the two vessels in Test 21bis. While it is very difficult to estimate the accuracy of the film heat transfer in the simulations, the velocity of the falling film in the experiments can be roughly estimated and compared with the code predictions. In Test 9bis, condensation starts at around 2'900 s, close to the injection (where the steam concentration is higher), and the temperature drop at about one meter below occurs at about 4'000 s (Fig. 6). This suggests an experimental "average" velocity of the falling film of the order of 1 mm/s, which is one order of magnitude smaller than that calculated by the simulation without tuning the wall friction. It is therefore interesting to study if the basic modeling approach used by GOTHIC is inherently unable to predict falling film speed. A simplified adiabatic problem was then set-up for the film liquid flow along a vertical plane wall at standard atmosphere conditions with a prescribed mass flux close to that calculated for Test 9bis. Under steady-state conditions, the analytical solution for the vertical velocity in laminar flow (Bird et al., 1960) is:

$$V_z = \sqrt[3]{\frac{g\,\Gamma^2}{3\rho\mu}}$$

where Γ is the liquid mass flux and the other symbols have the usual meaning. For the conditions investigated (pressure=1 bar; T=298 K, Γ=0.0004 kg/m s, Re=15), the equation above gives a value of 8 mm/s. The calculation with GOTHIC using the same size of the mesh used for the analysis of the tests in PANDA resulted in an average speed of the liquid (the instantaneous speed having step changes and most of the time below 10 mm/s) within 50% of the analytical value. This result suggests that the discrepancy with the experiment is not likely to be related to the coarse modeling of the condensate liquid film (unresolved), but is due to the lack of some basic modelling feature for the flow wetting a dry, heated surface.

A preliminary survey of available work in this area revealed that not much is known, and the models used in other codes are based on uncertain physical background. In this respect it is worth mentioning that the approach used in the CONTAIN code (NUREG, 1997) for the run-down liquid film includes the limitation that, if the liquid film is thinner than 0.5 mm, this does not move and remains hanging to the wall. There is no justification given for this limitation. Research on falling films has produced a considerable amount of both theoretical and experimental information, especially in relation to adiabatic conditions. These investigations aimed mainly at obtaining statistical characteristics of falling films (thickness, velocity, wave velocity) as well as the threshold for transition from laminar to turbulent flow under various conditions. A recent example of these studies is given in Ambrosini et al. (2005), where the flow of a falling film at various temperatures and plate inclinations was investigated. In that study, partial wetting was not addressed and the results provided data on one-dimensional, wavy films on a completely wet wall. The wetting rate of an initially dry surface by an evaporating film has been extensively studied for hot surfaces (temperatures above the Leidenfrost temperature) in connection to the cooling of fuel rods, little has been done for the conditions of interest in containment applications, i.e., small wall-to-fluid temperature differences. The spreading of the fluid on a vertical plane has been studied, e.g. in Gonzalez et al. (2004), where, however, the conditions studied were adiabatic. The flow of a liquid film down an initially dry vertical plate has also been studied in relation to the break-up and formation of rivulets and dry patches (El Genk and Saber, 2001 and 2002). There the main focus was to determine the minimum wetting rate (liquid flux) that permits a uniform advancement of the leading edge of the liquid film. Below this threshold, an evaporating liquid film breaks in stable liquid rivulets. This information is related to the problems discussed in this paper but additional study is needed to determine whether the conditions studied are relevant for the condensation rates expected in reactor containment applications. For Test 21bis, there is no evidence that the code predicted a too fast propagation of the film. On the contrary, the correct timing of the large wall temperature drop at an elevation half way between the IP and the injection (Andreani et al., 2008) seems to indicate that the falling speed of the film was reasonably well predicted, at least initially. The key issue for this test was then the modeling of heat transfer from the

wall, which in the framework of GOTHIC as well as in other containment codes is tackled by means of semi-empirical approaches. A completely mechanistic description of the process (such as one that might be attempted by a CFD code) would necessitate, among other capabilities, the correct prediction of:

- 2-D mapping of the thickness of the film
- Interfacial mass/heat transfer
- Convective heat transfer from the wall to liquid and gas
- Formation of dry patches and hanging (steady) films
- Wetting of dry areas

In principle, a detailed multiphase CFD approach might be able to simulate the first three phenomena with a sufficiently fine grid. However, for the last two processes microscopic phenomena are expected to control the advancement of the triple interline (solid/liquid/gas) at the leading edge of the film, and adequate closure models are required. To the best of the authors' knowledge, experimental information and theoretical work on the evaporation of condensate film wetting a dry, heated vertical wall is not available.

6 CONCLUDING REMARKS

The analyses of two tests in PANDA with the GOTHIC code revealed an unexpectedly large role played by the distribution and re-evaporation of condensate liquid on the fluid temperature and steam concentration in horizontally connected vessels. Although the specific modelling features of GOTHIC may have an influence on the relative importance of this phenomenon in Test 21bis, the analyses and the parametric studies made, and the comparison with the experimental steam concentrations (Andreani et al., 2008) suggests that the magnitude of the interfacial mass transfer was in the right range. Therefore, the sensitivity of the results to the density differences resulting from the liquid film propagation and vaporization process can be considered, to a certain extent, independent of the code used. It can be concluded from these studies that the impact on the run-down of the liquid film and the associated heat/mass transfer could be of some importance in containment analyses, and adequate models should be implemented in containment and CFD codes. On the other hand, it seems that some fundamental knowledge on the basic thermal-hydraulic processes governing the run-down of a liquid film is missing, and additional future research is needed to address this issue.

ACKNOWLEDGMENTS

The authors gratefully acknowledge the support of all the countries and the international organizations participating in the OECD/SETH project, and particularly of the members of the Management Board and the Programme Review Group of the SETH project. The authors would also like to thank Dr. Peter Royl (FZK) for the helpful discussions and for comparing the results obtained here with the GOTHIC code with his results with the GASFLOW code.

REFERENCES

Ambrosini, W, Forgione, N, Oriolo, F. (2002), " Statistical Characteristics of a Water Film Falling Down a Flat Plate at Different Inclinations and Temperatures', Int. J. Multiphase Flow, Vol. 28, pp. 1521-1540.

Andreani, M. (2003), "On the Use of the Standard k-ε Model in GOTHIC to Simulate Buoyant Flows with Light Gases", The 10th International Topical Meeting on Nuclear Reactor Thermal Hydraulics (NURETH-10), Seoul, Korea, 5-9 October 2003, CD-ROM paper E00005.

Andreani, M., Putz, F., Dury, T.V., Gjerloev, C., Smith, B.L. (2003), "On the Application of Field Codes to the Analysis of Gas Mixing in Large Volumes: Case studies using CFX and GOTHIC", Annals of Nuclear Energy, Vol. 30, pp. 685-714.

Auban, O., Paladino, D., Zboray, R. (2005), "PANDA Test Facility Description and Geometrical Data", PSI internal Report TM-42-05-06; ALPHA-05-01-0.

Andreani, M., Paladino, D., George, T. (2008), "Simulations of Basic Gas Mixing Tests with Condensation in the PANDA Facility using the GOTHIC code", paper to be presented at the 16th Int. Conference on Nuclear Engineering, ICONE16, paper 48917, Orlando, FL, USA, May 12-15, 2008.

Bird, R.B., Stewart, W.E. and Lightfoot E.N. (1960), Transport Phenomena, Wiley Int. Ed., pag. 40.

de Cachard, F., Paladino, D., Zboray, R., Andreani, M. (edited by Huggenberger, M.) (2007), "OECD-SETH Project Large-scale Experimental Investigation of Gas Mixing and Stratification in LWR Containments", PSI internal Report TM-42-07-04; ALPHA-07-18-A.

Dreier J. et al. (1996), "The PANDA Facility and First Results", Kerntechnik, Vol. 61, pp. 214-222.

El-Genk, M. and Saber, H.H. (2001), "Minimum Thickness of a Flowing Down Liquid Film on a Vertical Surface", Int. J. Heat Mass Transfer, Vol. 44, pp. 2809-2825.

El-Genk, M. and Saber, H.H. (2002), "An Investigation of the Break-up of an Evaporating Liquid Film, Falling Down a Vertical, Uniformly Heated Wall", J. Heat Transfer, Vol. 124, pp. 39-50.

Gonzalez, A.G., Diez, J., Gomba, J., Gratton, R., Kondic, L. (2004), "Spreading of a thin two-dimensional strip of fluid on a vertical plane: experiments and modeling", Physical Review E, Vol. 70, 026309-1.

GOTHIC Containment Analysis Program, Version 7.2a(QA), EPRI, Palo Alto, CA, Jan. 2006.

NUREG-0588, Rev. 1 (1980) "Interim Staff Position on Environmental Qualification of Safety-Related Electrical Equipment", Nov. 1980.

NUREG/CR-6533 (1997), "Code Manual for Contain 2.0: A Computer Code for Nuclear Rector Containment Analysis", SAND-1735, 1997.

Paladino, D., Auban, O., Zboray, R. (2006), "Large scale Gas Mixing and Stratification Triggered by a Buoyant Plume with and without Occurrence of Condensation", Proceedings of the 9th International Congress on Advances in Nuclear Power Plants (ICAPP '06), Reno, NV, USA, 4-8 June, 2006.

Yadigaroglu, G., Andreani, M., Dreier, J., Coddington, P. (2003), "Trends and needs in experimentation and numerical simulation for LWR safety", Nuclear Engineering and Design, Vol. 221, pp. 205-223.

Zboray, R., Paladino, D., Auban, O. (2006), "Experiments on gas mixing and stratification driven by jets and plumes in large-scale, multi-compartment geometries", Proceedings of 14th International Conference on Nuclear Engineering (ICONE-14), Miami, Florida, 17-20 July, 2006.